Specificities of Rich Spray-Flame Spreading

Colette Nicoli, Pierre Haldenwang, Bruno Denet

Specificities of Rich Spray-Flame Spreading

C. Nicoli[1], P. Haldenwang[1], B. Denet[2]

[1] M2P2 , AMU/ CNRS/ Centrale Marseille , UMR 7340, 13451 Marseille France
[2]IRPHE, AMU/ CNRS/Centrale Marseille , UMR 7342, 13451 Marseille France

Abstract

This study concerns two-phase flame propagating through a 2D-lattice of alkane droplets surrounded by a gaseous pre-mixture of alkane air. Spray flame speed is numerically measured for spray compositions. To study such very heterogeneous media, the retained chemical scheme is a global irreversible one step reaction governed by Arrhenius law, with a modified heat of reaction depending on local equivalence ratio. Studied sprays are globally rich. For global equivalence ratio greater than 1.4, and lattice spacing large enough, the presence of droplets promotes combustion (in comparison with single phase flame dynamics). When the vapor pressure becomes important, droplets do not participate to combustion. These numerical results are in qualitative good agreement with recent experimental contributions on spray combustion.

Nomenclature

$F(\varphi)$ heat of reaction depending on equivalence ratio
Le_i Lewis number of species i in the mixture
L_x , L_Y longitudinal and transversal box lengths
P_{e_s} spray Peclet number
U_L adiabatic speed for single-phase premixed flame
U_L^* adiabatic flame speed for stoichiometric gaseous mixture
U_s spray-flame speed
s Vlattice spacing
T_b adiabatic flame temperature for stoichiometric gaseous mixture
Z mixture fraction
Z_e Zeldovich number for stoichiometric gaseous mixture
φ_u local equivalence ratio
φ_L liquid equivalence ratio of the fresh spray (overall liquid loading)
φ_G gaseous equivalence ratio of the fresh spray
φ_T overall equivalence ratio of the fresh spray
θ reduced temperature
Ψ_i reduced mass fraction of specie i

Introduction

This works deals with the dynamics of rich two-phase flames. Combustion experiments in sprays at high pressure have revealed behaviours in large departure from the equivalent gaseous premixed flames. The part played by droplet size has clearly been evidenced. Recent microgravity experimental results by Nassouri et al. and Thimothee et al. [1-3] indicated that spray-flame is much more unstable than the equivalent single-phase flame. In the classical ground experiments conducted by Hayashi et al. [4] in Wilson chamber, the spray-flame speed measurements had already shown a displacement of the rich flammability limit towards higher equivalence ratio. Recent similar experiments by Bradley et al. [6] in Wilson chamber confirm these trends, and even indicate that increasing liquid loading for very large droplets does not strongly modify the spray-flame speed. Among the earliest experiments on spray-flames, on the rich side $U_S(\varphi_T)$, the spray-flame speed is found larger than $U_L(\varphi_T)$, the single-phase flame of the same overall equivalence ratio. An explanation for this velocity increase has been proposed by Hayashi and Kumagai [4-5] : the spray-flame speed is simply $U_L(\varphi_G)$, the velocity of the premixed 1-phase flame with the equivalence ratio of the gaseous surrounding mixture. In other words, droplets do not participate to propagation. Another possible cause for spray-flame speed enhancement, clearly observed in the experiments particularly at high pressure [6-7], is that spray-flames are subjected to front instabilities, whereas 1-phase flames remain planar in the same conditions.

The present numerical study aims to interpret the increase of spray-flame speed observed on the rich side and to look at the specific role of the droplets on the flame front structuration. This work is devoted to large transversal length, L_Y, of the computational box for which the flame front becomes unstable with respect to Darrieu-Landau (DL instability). Recent work [17] has proved that spray-flame speed promotion on the rich side can be seen as an intrinsic effect, as soon as the droplet size is large enough.

The configuration of spray presently studied consists in schematizing the initial unburnt two-phase medium thanks to a centered 2D-lattice of heavy alkane droplets surrounded by vapour pressure and air (see Fig. 1). In the spirit of the effect sought after, the droplet inter-distance (or lattice spacing s) is considered to be large in comparison with the characteristic reaction-diffusion scale. In other words, s is here supposed to be too large for modelling combustion through some homogenization process [8-9]. In such a configuration, φ_u, the local equivalence ratio of the fresh mixture, can vary from a very rich (large) value close the droplets to the equivalence ratio far from the droplets (i.e. that due to the vapour pressure in the mixture), hereafter denoted by φ_G. In the same manner, φ_L expresses the equivalence ratio of

the fuel under liquid phase (or liquid loading), while φ_T (with $\varphi_T = \varphi_G + \varphi_L$) is the overall equivalence ratio .

Because combustion spreads in a medium of variable composition, a chemical scheme taking account of the local equivalence ratio in the unburnt mixture has been developed [10]. This (simplest) model retains a global irreversible one-step reaction, governed by an Arrhenius law, the heat reaction of which depends on φ_u . In other words, heat release takes account of all the species existing at the actual flame temperature [10].

The spray flame speed is determined as a function of the overall equivalence ratio or the liquid loading (i.e the droplet radius effect), when the rich gaseous mixture is fixed at is considered $\varphi_G = 1.1$, in a large computational domain $L_Y = 48$ (with the lattice spacing ($s = 24$).

Modelling Spray-Flame

The present numerical modelling uses the usual set of conservation laws: mass, momenta, energy and species. Since the accurate chemical schemes for alkane are too complex for efficient simulations, a standard approach for a heterogeneous medium considers a simplified chemical kinetics. The simplest manner consists of choosing an irreversible 1-step reaction, the parameters of which are adjusted to mimic the actual flame temperature and dynamics.

It is known that the classical one-step Arrhenius law largely overestimates the adiabatic flame temperature in the rich side. To overcome the difficulty of assessing the main flame characteristics correctly, a modification [10] of the standard chemical scheme is considered: heat release becomes a linear function $F(\varphi_u)$ of the fresh pre-mixture equivalence ratio φ_u . $F(\varphi_u)$ is adjusted to mimic the premixed single-phase flame behaviours (adiabatic flame temperature and flame speed) [10]. As for the estimate of φ_u , two combustion invariants allow us to derive φ_u from any (burnt or unburnt) point-wise mixture composition [15].

Non-dimensioning

Non-dimensioning is performed with the use of the theoretical data related the stoichiometric (gaseous) premixed flame as derived in the theoretical papers by Joulin and Mitani [11] and Garcia-Ybarra et al. [12]. The stoichiometric flame temperature, as T_b^*, is given by

$$T_b^* = T_u + \frac{(Y_f)_u^* Q}{C_p \nu_f M_f}$$

Temperature and species mass fractions are handled under the reduced forms

$\theta = (T - T_u)/(T_b^* - T_u)$; $\psi_i = Y_i / Y_{i,u}^*$

(i=f for the alkane and i=o for oxygen)

As for the time and length scales, we use $D_{th,b}^*$, the thermal diffusivity coefficient of the burnt gases, and the stoichiometric (gaseous) flame speed as given by

$$(U_L^*)^2 = \frac{4}{Ze^3}\left(\frac{\rho_b^*}{\rho_u^*}\right)^2 \frac{\lambda_b}{\rho_b^* C_p}\left[(\rho_b^*)^2 \nu_f M_f Y_{o,u}^* B_b\right]\exp(-T_A / T_b^*)$$

Heterogeneous Medium and Combustion model

This allows us to establish the scalar conservation laws under the following dimensionless form

$$\frac{\partial \theta}{\partial t} + \overline{V}.\overline{\nabla}\theta = \frac{1}{\rho C_p} div(\lambda \overline{\nabla}\theta) + \mathrm{F}(\varphi_u)\, W(\rho, \psi_i, \theta)$$

$$\frac{\partial \psi_i}{\partial t} + \overline{V}.\overline{\nabla}\psi_i = \frac{1}{\rho} div(\rho D_i \overline{\nabla}\psi_i) - \nu_i M_i W(\rho, \psi_i, T)$$

where the reaction rate is now defined as

$$\mathrm{W}(\rho, \psi_i, \theta) = \frac{Ze^3}{4}\left(\frac{\rho_u^*}{\rho_b^*}\right)^2 \psi_f \psi_o \left[\frac{\rho}{\rho_b^*}\right]^3 exp\left[Ze\frac{\theta - 1}{1 + \gamma(\theta - 1)}\right]$$

with the reduced activation energy (Zeldovich number) $Ze = T_A(T_b^* - T_u)/(T_b^*)^2$ and $\gamma = (T_b^* - T_u)/T_b^*$. As in the conservation laws appears the velocity field $\overline{V}$, the reaction-diffusion system is coupled with the Navier-Stokes equations. The overall scheme that computes the Navier-Stokes equations has previously been described in Denet and Haldenwang [13]. Accordingly with the above non-dimensioning, the general form given to the adjustment function $F(\varphi_u)$ can be approximated by the following quantity

$F(\varphi_u) = [1 - \alpha(\varphi_u - 1)]$ if $\varphi_u \in [0.5, 2]$,

whereas $W = 0$ if $\varphi_u < 0.5$ or $\varphi_u > 2.$.

α is a coefficient depending on the fuel. For octane-air pre-mixtures, $\alpha = 0.33$ and $Ze = 7$ have been chosen from experimental data [10].

In what follows, the x-coordinate corresponds to the direction of propagation of a folded flame front. To define the mean position of this front, we perform an averaging in the transverse (y) direction of the temperature field to get $<\theta>_y (x)$. By definition, x_F, the front position, is given by $<\theta>_y (x_F) = 0.5$.

Results: Spray-Flame spreading in transversally large computational domain

The numerical simulations have been carried out using the following parameters: the Lewis number of fuel, oxygen and nitrogen are respectively $Le_F = 1.8$, $Le_O = 0.9$, $Le_N = 1$. The overall equivalence ratio φ_T is varied in the rich range $[1.6, 3]$. The spray flame front position, and consequently the spray flame speed, is assessed by

following a given isotherm, $<\theta>_y (x_F) = 0.5$, as in[15].

In a general manner, combustion spreading is found to be not uniform in time: it combines stages of vaporization and stages of flame propagation (see figure 4). The high-level of non- homogeneity in a spray flame and the complexity of the spreading are illustrated in figures 1 and 2.

Figures 2 represent two fields at three instants in the spray flame soon after the ignition up the consumption of the first droplets.

When ($L_Y > 14$), the computational box is large enough to allow the front to develop wrinkles, if initial perturbations are introduced. For the sake of an easy interpretation of the numerical results, we keep the spray Peclet number large enough to maintain the spray-flame in the Hayashi-Kumagai (HK) regime [17]. The spray Peclet number $Pe_s\left[U_L(\varphi_G)\right]$ is defined as the ratio of the droplet vaporization time on the propagation time (through the lattice spacing at the speed $U_L(\varphi_G)$)

We decide to choose the initial spray parameters in such manner that $4. \le Pe_S \le 15.5$. More precisely, the composition of the spray, has a fixed gaseous pre-mixture $\varphi_G = 1.1$ and the global equivalence ratio is in the range $1.6 \le \varphi_T \le 3$. The parameter of the study is φ_T (and concomitantly R_d) Typical spray example is given in Fig.1, where ignition is performed at right hand side of the computation domain and propagation occurs from the right to the left.

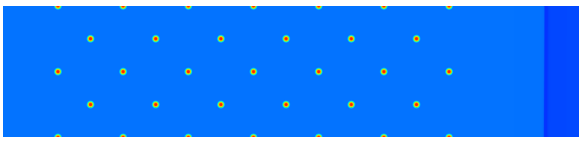

Figure 1. Initial fuel mass fraction: dark blue zone (on the right hand edge) indicates gases already burnt; flame then spreads to the left,
$\left(L_X = 233\ ;\ L_Y = 48\ \ ;\ s = 24\ ;\varphi_G = 1.1\ ;\ \varphi_T = 2\ ;\ R_d = 1.48\right)$

As mentioned above, the computational domain of Fig.1 is transversally large enough to sustain DL instability. The retained value of the transversal box length is $L_Y = 48$. As ignition is carried out in the single-phase pre-mixture, DL instability classically develops as a cusped front. Then, the cusped pattern meets the successive rows of droplets.

To illustrate the interaction between the DL affected premixed flame with the spray droplets, we have plotted in figures 2, three successive snapshots of the fuel mass fraction field and reaction rate field. As in our model the droplets can move, they are carried along, and stretched, by the flow (to the right) due to vaporization and gas expansion.

Fig.2a indicates that the droplets are transported by the flow back to the burnt gases much before their complete vaporization and mixing. This confirms that we are faced with the Hayashi-Kumagai (HK) regime of spray-flames. We note the classical cusped pattern of the flame front with a large length scale that corresponds to $L_Y = 48$. The main cusped pattern of the reaction rate is marked by additional wrinkles of smaller length scales due droplets.

Figures 2: Alkane air mixture: $\varphi_T = 2.$, $\varphi_G = 1.1$, $\varphi_L = 0.9$ and $\left(L_Y = 48\ ;\ s = 24\right)$

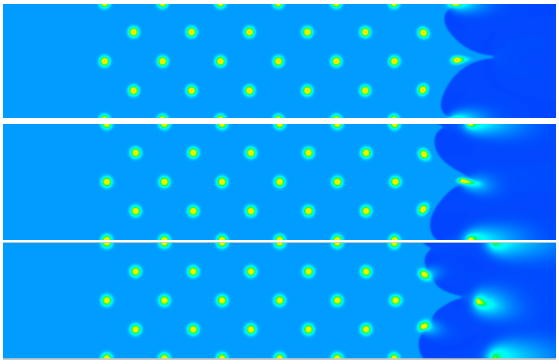

Fig 2a. Fuel mass fraction field at three instants after the ignition.

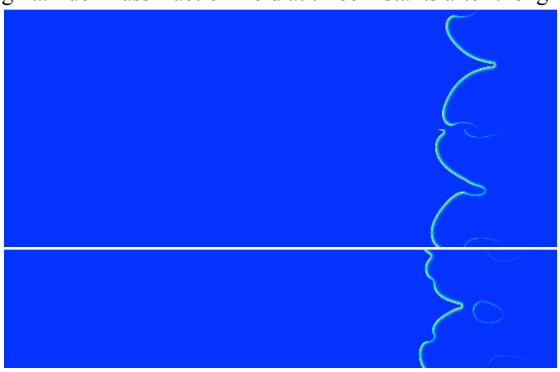

Fig 2b. Production term at three instants after the ignition.

To illustrate the further development of the DL instability, 20 successive snapshots of the reaction rate field are drawn in Fig.3.a. Two successive snapshots are separated by the time interval $\Delta t = 7.12$. For the sake of comparison with the averaged front position x_F -which as been defined above- $x_F(t)$ is plotted in Fig.3.b. When comparing Fig.3.a and Fig.3.b, this slope allows us to assess the mean front velocity that corresponds to every reaction rate profile.

At time t=32, in Fig.3.b a change in the slope of the position curve is observed. This indicates that the DL affected flame meets the spray. In other words, in the range $0 \le t \le 32$ the development of the (classical) Darrieus-Landau instability in a single-phase pre-mixture is observed. At the end of this time laps, the speed-up of

the flame has enhanced the flame speed from $U_L(\varphi_G = 1.1) = 0.99$ to $U_{DL}(L_Y = 48) = 1.1$, the single-phase flame speed affected by DL instability.

After time t=32, the cusped form of the front becomes more corrugated because the flame meets the droplets and we are faced with a spray-flame in the HK regime. A spray-flame speed-up again occurs as shown by Fig.3.b. When the spray-flame leaves the last row of droplets, the spray-flame speed is $U_S(L_Y = 48) = 1.47$.

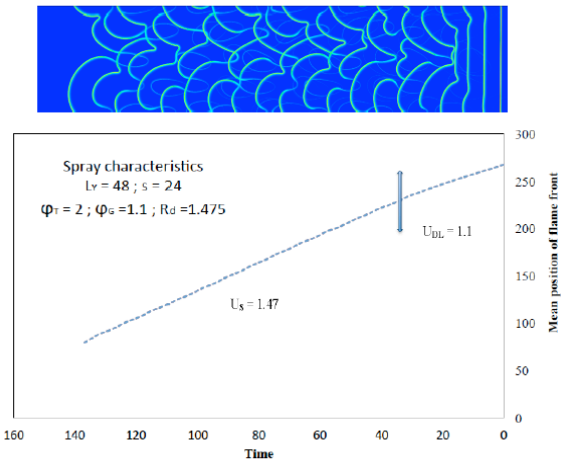

Figures 3: Spray-flame affected by Darrieus-Landau instability

$\varphi_T = 2.,\ \varphi_G = 1.1,\ \varphi_L = 0.9\ \ (L_Y = 48\ ;\ s = 24;\ R_d = 1.47)$

a) Superimposition of successive snapshots of the reaction rate field

(b) Mean x-position of the combustion front vs. (time) : spray-flame speed is given by the slope of the curve.

Figures 3 illustrate a case of a spray flame spreading in the Hayashi-Kumagai (HK) regime, submitted to the DL instabilities. It appears that spray-flame speed is larger than $U_{DL}(\varphi_G = 1.1)$: the promotion on the rich side can be seen as an intrinsic effect, due to the fact that the droplet size is large enough [17].

Droplet radius influence on the spray flame speed.

On figure 4, the spray flame position of quite a few spray mixtures (global equivalence ratio φ_T or droplet radius) versus the time are compared. φ_T The mean slope of the curves gives is the spray flame speed. Until time (t=32), the flame front of each studied spray crosses a purely gaseous pre-mixture $\varphi_G = 1.1$ in a large box: the flame position versus time is the same for each spray mixture. After t=32, when the flame front meets the droplets, it can be observed that small differences exist: spray flame is faster for the smallest droplets. For larger values of φ_T, ie the greater droplets (ie, $R_d \geq 2$), droplets in the mixture still boost the flame front, but larger droplets are, smaller the spray flame speed is.

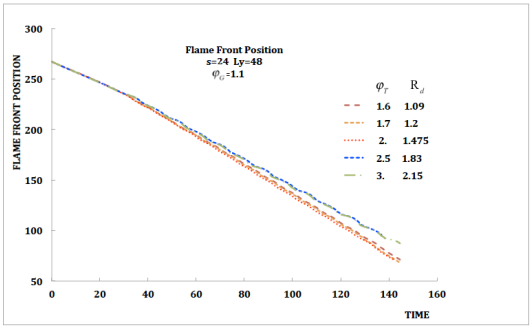

Figure 4 : Flame front position versus the time for various global equivalence ratio (or various droplet radius)

$(L_X = 300\ ;\ L_Y = 48\ \ ;\ s = 24\ ;\ \varphi_G = 1.1)$

On figure 5, the spray flame speed versus droplet radius, shows that as soon as $R_d \leq 1.5$, spray flame speed is about $U_s \approx 1.45$, while if $R_d \geq 1.8$, $U_s \approx 1.33$.

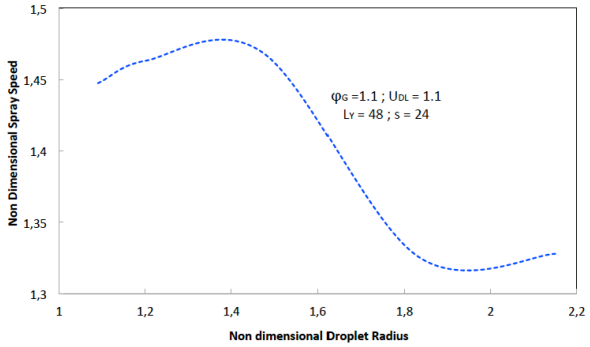

Figure 5: Spray flame speed versus droplet radius

$(L_X = 300\ ;\ L_Y = 48\ \ ;\ s = 24\ ;\ \varphi_G = 1.1)$

The DL instability of the spray-flame -in the HK regime- provokes a stronger speed-up. The great difference between rich spray flame speed and equivalent premixed gaseous flame speed is undoubtedly due to the role of the droplets that bring additional wrinkles to the DL-affected flame front and still accelerate the flame for large enough droplet. This acceleration has not a monotone dependence on the droplet radius.

To sum up this numerical study, in Table 1 we have gathered the spray-flame speed when the DL instabilities are developed, for various rich global equivalence ratio. The first line corresponds to a droplet radius for each spray. The second line is the spray Peclet number $Pe_s\left[U_L(\varphi_G)\right]$ defined as the ratio of the droplet

vaporization time on the propagation time (through the lattice spacing at the speed $U_L(\varphi_G)$)

All the cases studied have a very large $Pe_s\left[U_L(\varphi_G)\right]$:

but, when $Pe_s\left[U_L(\varphi_G)\right] \leq 10$ droplets are more efficient to contribute at the acceleration of the spray flame. An optimal droplet size seems to exist to increase the flame front wrinkling.

φ_T	1.6	1.7	2	2.5	3
R_d	1.09	1.2	1.475	1.83	2.15
$Pe_s\left[U_L(\varphi_G)\right]$	4	4.84	7.3	11.27	15.5
U_s	1.44	1.46	1.47	1.32	1.33

Table 1. Spray-flame speed U_s for various values of R_d

$\varphi_G = 1.1$, $L_Y = 48$ and s =24 ; $U_L\left(\varphi_G = 1.1\right) = 0.99$

Conclusion

This numerical study on rich spray combustion presents the influence of global spray composition (liquid loading, or droplet radius) on spray-flame speed, with a quasi-stoichiometric gaseous pre-mixture in a large computational domain. The spray flame speed is larger than the speed of the purely gaseous flame with an equivalent equivalence ratio. Purely DL instabilities can develop and increase the flame front surface. In a second time, other wrinkles due to the droplet are added: a new acceleration , depending of the droplet size exists.

Acknowledgements

This study was granted by the Research Program " Micropesanteur Fondamentale et Appliquée "- GDR 2799 - CNRS/CNES under the contract CNES/140569.

References

1. M. Nassouri, C. Chauveau, F. Halter, I. Gökalp, "Combustion of aerosols: structure and speed flame study in microgravity". Proceedings of the European Combustion Meeting 2013 (ECM), 25-28 June 2013, Lund, Sweden.
2. R. Thimothee, C. Chauveau, F. Halter, I. Gokalp, Rich spray-flame propagating through a 2d-lattice of alkane droplets inair, Proceedings of ASME Turbo Expo 2015: Turbine Technical 445 Conference and Exposition GT2015, 2015
3. Thimothee R., Chauveau C., Halter F., C. Nicoli, P. Haldenwang, B. Denet , "Microgravity experiments and numerical studies on ethanol/air spray-flames." Comptes-Rendus Mécanique; in press (2016)
4. S. Hayashi, S. Kumagai and T. Sakai, Propagation velocity and structure of flames in droplet-vapor-air mixtures, Combust. Sci. and Tech., 15: 169-177, 1976.
5. S. Hayashi, S. Kumagai, , Flame Propagation in Fuel Droplet-Vapor-Air Mixtures. Proc Combust Institute., 15,445-451, 1975.
6. D.Bradley, M. Lawes, S.Y. Liao, A Saat.. Laminar Mass burning and entrainment velocities and flame instabilities of isooctane, ethanol and hydrous ethanol/air aerosols. Combust. and Flame , 161:6, pp. 1620–1632, 2014.
7. H. Nomura, I. Kawasumi, Y. Ujiie, J. Sato, Effects of pressure on propagation in a premixture containing fine fuel droplets, Proc. Combust. Inst. 31 (2007) 2133-2140.
8. Suard S., Haldenwang P. and Nicoli C., "Different spreading regimes of spray-flames", C. R. Mécanique, vol. 332 (5-6), pp. 387-396 (2004)
9. Nicoli C., Haldenwang P. and Suard S., "Analysis of pulsating spray flames propagating in lean two-phase mixtures with unity Lewis number", Combustion & Flame, vol. 143, pp. 299-312 (2005)
10. C. Nicoli, P. Haldenwang, Analysis of one-step chemistry models for flame propagation in various equivalence ratio premixtures of high alkane-air, SPEIC10: Towards Sustainable Combustion, Tenerife, June 2010.
11. G. Joulin, and J. Mitani, Linear stability analysis of two-reactant flames, Combustion and Flame, Vol. 40, pp. 235-246 , 1981.
12. P. Garcia-Ybarra, C. Nicoli, P. Clavin , Soret and Dilution Effects on Premixed Flames, Combust. Sci. Tech, Vol. 42 , pp. 87-109, 1984.
13. B. Denet, P. Haldenwang, A numerical study of premixed flames Darrieus-Landau instability. Combust. Sci. Techn., Vol. 104, pp. 143-16, 1995.
14. C. Nicoli, B. Denet, P. Haldenwang. Lean flame dynamics through a 2D lattice of alkane droplets in air. Combust. Sci. and Tech., 186: 2, pp. 103-119, 2014.
15. C. Nicoli, B. Denet, P. Haldenwang., "Rich Spray-Flame Propagating through a 2DLattice of Alkane Droplets in Air", Combustion & Flame, Vol. 162(12), pp. 4598-4611 (2015)
16. C. Nicoli, P. Haldenwang, B. Denet. "Spray-Flame Dynamics in a Rich Droplet Array" Flow Turbulence & Combustion; Vol. 96, pp. 377–389 (2016)
17. C. Nicoli, P. Haldenwang, B. Denet. "Darrieus-Landau instability of premixed flames enhanced by fuel droplets." Combustion Theory and Modeling ; accepted for publication http://dx.doi.org/10.1080/13647830.2017.127975